Modelling DTPA therapy following Am contamination in rats

Manuel Kastl, Olivier Grémy, Stéphanie Lamart, Augusto Giussani, Wei Bo Li, Christoph Hoeschen

Title: Modelling DTPA therapy following Am contamination in rats

Manuel Kastl[1], Olivier Grémy[2], Stephanie Lamart[3], Augusto Giussani[4], Wei Bo Li[1, 4], Christoph Hoeschen[5]

[1]Institute of Radiation Medicine, Helmholtz Zentrum München - German Research Center for Environmental Health, Neuherberg, Germany

[2] Laboratoire de Radio Toxicologie, CEA, Université de Paris-Saclay, Arpajon, France

[3] Institut de Radioprotection et de Sûreté Nucléaire (IRSN), PSE-SAN/SDOS/LEDI, Fontenay-aux-Roses, France

[4] Division of Medical and Occupational Radiation Protection, Federal Office for Radiation Protection, Neuherberg, Germany

[5] Institut für Medizintechnik, Otto-von-Guericke University Magdeburg, Magdeburg, Germany

Corresponding author:

Manuel Kastl

manuel.kastl@helmholtz-munich.de

Phone: +49 (0) 163 3797156

Keywords: Chelation, DTPA, Americium, Biokinetic Model, Decorporation

Author contributions: Conceptualization: MK, AG; Methodology: AG, MK, OG, SL; Data collection: OG; Formal analysis and investigation: MK, AG; Writing - original draft preparation: MK; Writing - review and editing: all authors; Supervision: CH

Acknowledgements: The authors would like to thank the numerous colleagues from the EURADOS working group WG7 “Internal dosimetry”, especially the ones working in the task group “DTPA chelation modelling” for their contributions and fruitful discussions throughout the years.

Abstract

A major challenge in modelling the decorporation of actinides (An), such as americium (Am), with DTPA (diethylenetriaminepentaacetic acid) is the fact that standard biokinetic models become inadequate for assessing radionuclide intake and estimating the resulting dose as DTPA perturbs the regular biokinetics of the radionuclide. At present, most attempts existing in the literature are empirical and developed mainly for the interpretation of one or a limited number of specific incorporation cases. Recently, several approaches were presented with the aim of developing a generic model, one of which reported the unperturbed biokinetics of plutonium (Pu), the chelation process and the behaviour of the chelated compound An-DTPA with a single model structure. The aim of the approach described in this work is the development of a generic model, that is able to describe the biokinetics of Am, DTPA and the chelate Am-DTPA simultaneously. Since accidental intakes in humans present many unknowns and large uncertainties, data from controlled studies in animals were used. In these studies, different amounts of DTPA were administered at different times after contamination with known quantities of Am. To account for the enhancement of faecal excretion and reduction in liver retention, DTPA is assumed to chelate Am not only in extracellular

fluids but also in hepatocytes. A good agreement was found between the predictions of the proposed model and the experimental results for urinary and faecal excretion and accumulation and retention in the liver. However, the decorporation from the skeletal compartment could not be reproduced satisfactorily under these simple assumptions.

1. Introduction

The incorporation of actinides (An), e.g., plutonium (Pu) or americium (Am), can cause severe health damage due to the continuous alpha irradiation of organs and tissues such as the lungs, liver and skeleton, where they can be retained for decades (ICRP 2019). Treatment with the chelating agent DTPA (diethylenetriaminepentaacetic acid) as a salt of calcium (Ca) or zinc (Zn) is the commonly used therapy to remove Pu/Am from the body (Ménétrier et al. 2005; Grappin and Bérard 2008; Grappin et al. 2006, 2007a, b; 2008, 2009). Indeed, the injection or inhalation of Ca/Zn-DTPA enhances the excretion of the incorporated actinide by forming stable An-DTPA chelates, thus minimizing the amount of An retained in the body and the resulting committed effective dose.

The basic principle of decorporation therapy with chelating agents is described in (Kety 1942) and has been applied since the 1950s (Catsch 1968; Volf 1978). Ca-DTPA has been approved for the treatment of Pu/Am incorporation in in many countries, e.g., in the USA (FDA 2015), France (Grappin and Bérard 2008) and Germany (approved in 2005, marketing authorization number 6813281.00.00[1]). Numerous animal studies and human studies have provided evidence about the efficacy of DTPA treatment (Volf 1978; Catsch 1968; Roedler et al. 1989; Carbaugh et al. 1989; Grémy et al. 2016; Jech et al. 1972; Fisher 2000; Bhattacharyya et al.1992; Bertelli et al. 2010; Bertelli et al. 2018; Breustedt et al. 2019; Cohen et al. 1974; Davesne et al. 2016; Hengé-Napoli et al. 2000; Grappin et al. 2006; Gorden et al. 2003; Durbin et al. 2006; Stradling et al. 2000; Fritsch et al. 2007; James et al. 2007; Jolly et al. 1972; Poudel et al. 2017; Schadilov 2010; Schadilov et al. 2005; Schofield and Lynn 1973; Norwood 1960; Ohlenschläger et al. 1978; Grémy et al. 2021; Lamart et al. 2021). Side effects and complications associated with DTPA treatments are not uncommon (Taylor et al. 2007; Glover et al. 2022).

Usually, the dose after the incorporation of radionuclides is estimated by interpreting direct measurements of the activity in the body or by measurements of the excreted activity using compartment models. These models provide a mathematical method to predict the distribution and excretion patterns of the radionuclides in the body (ICRP 2015).

In the case of chelation therapy, the complexation between the chelating agent and actinide perturbs the characteristic biokinetic behaviour of the actinide because the resulting An-DTPA chelate is very readily and rapidly excreted. Consequently, the existing reference biokinetic models, such as those published by the International Commission on Radiation Protection (ICRP 2019), become inadequate for interpreting bioassay measurements after the administration of DTPA, estimating the incorporated activity and assessing the success of the therapy in terms of averted dose.

However, estimates of the incorporated activities and of the resulting doses are necessary for planning individually adapted therapies. This can be achieved with a generic model able to predict the effects of DTPA on the biokinetics of actinides depending on e.g. the type, amount and schedule

[1] The summary of product characteristics for Ditripentat-Heyl®, including information on its authorization in Germany, can be accessed by making a search in the database of the Federal Office for Drugs and Medical Devices (Bundesinstitut für Arzneimittel und Medizinprodukte), accessible through this link: https://www.pharmnet-bund.de/dynamic/en/drug-information-system/index.html, search term: Ditripentat

of administration. The optimization of the treatment protocols involves balancing the gains in terms of the averted dose and the resulting health benefits for the contaminated persons with the efforts needed for performing the therapy, including financial costs, time burden, as well as discomfort and side effects for the treated individuals. Numerous modelling approaches are reported in the literature; however, most of them are case-specific and empirical and do not provide an explicit description of the chelation processes (Jech et al. 1972; Jolly et al. 1972; Poudel et al. 2017; Hall et al. 1978; LaBone 1994; LaBone 2002; Bailey et al. 2003; Fritsch et al. 2007; Fritsch et al. 2009; James et al. 2007; Breustedt et al. 2019; Sérandour and Fritsch 2008, 2009; Konzen et al. 2016). They are not suitable for general predictions of therapeutic success in connection with DTPA since these approaches are optimized for specific experimental results. Recent works based on human data pursued the aim of developing a generic model: Konzen and Brey (2015) provide a Pu-DTPA biokinetic model for the estimation of Pu intake, which can be used to evaluate several chelation strategies and, hence, derive some recommendations for effective treatment. Dumit et al. (2019) presented an attempt to provide a comprehensive description of the unperturbed biokinetics of Pu, the chelation process and the behaviour of the chelated compound Pu-DTPA with a single model structure using the so-called CONRAD approach, first described in Breustedt et al. (2009). This approach consists of modelling the biokinetic behaviour of the actinide, of the intravenously injected chelating agent and of the *in vivo* formed chelate as separate structures which are then coupled together by a suitable mathematical description of the chelation mechanism as a second-order process.

A major issue in modelling decorporation therapies with chelating agents is the difficulty in deriving information about the chelation site from the available data. To date, no mechanisms are known that would allow DTPA to cross the cell membranes and enter the cells. A frequently used assumption is therefore that DTPA is distributed only in the extracellular fluid (ECF). This approach is supported by the particularly high efficiency of DTPA therapies observed when DTPA was administered shortly after the accidental incorporation, while the actinide was still present in the plasma and ECF, and by the fact that more than 99% of DTPA was excreted from the body within the first day after injection (Breustedt et al. 2009, Stevens et al. 1978, Stather et al. 1983, Durbin et al. 1997).

On the other hand, several studies have indicated liver and skeletal decorporation of Pu/Am in animals (Bhattacharyya et al. 1978a, b; Bhattacharyya and Peterson 1979; Cohen et al. 1974; Fritsch et al. 2010; Grémy et al. 2016) and humans (Roedler et al. 1989; Fritsch et al. 2007; James et al. 2007; Grémy et al. 2021; Dumit et al. 2019) and reported an effectiveness of late treatment (Kety 1942; Roedler et al. 1989; Volf et al. 1999; James et al. 2007; Grémy et al. 2021), when the actinide is assumed not to be in the ECF any longer. Other animal studies documenting an increased biliary/faecal excretion of Pu/Am postulate that DTPA is able to penetrate the liver cell boundaries and suggest intracellular chelation (Schubert et al. 1961; Grémy et al. 2016; Markley et al. 1964; Ballou and Hess 1972; Bhattacharyya et al. 1978a, b; Bhattacharyya and Peterson 1979). Here, it should be noted that the amount of DTPA administered in animal studies generally by far (several orders of magnitude) exceeds the amount of actinide in terms of moles. Recent works from Dumit et al. have used a comprehensive amount of human data to develop and validate chelation models (Dumit et al. 2019a, b; Dumit et al. 2020a, b; Dumit et al. 2023). These publications show evidence of intracellular chelation in both skeleton and liver. The present work, however, uses animal data and it is not straightforward to reproduce and observe the same results obtained when using human data. Based on this evidence, the possibility that a very small fraction of DTPA is able to cross cell membranes and chelate material deposited there has been intensively discussed (Grémy et al. 2016; Fritsch et al. 2010; Grémy and Miccoli 2019; Grémy et al. 2021).

Alternatively, the increased faecal excretion might be explained by a mobilization of nonchelated actinides in the liver after DTPA administration (Hall et al. 1978), leaving the site of chelation as a fundamentally open question, which cannot be solved only based on data interpretation. However, the development of adequate biokinetic models can contribute to solving this question.

Human data are usually derived from accidental incorporation cases, for which the type and chemical form of the incorporated material are in general known only very roughly, if ever, and sometimes even the exact time of incorporation is unknown. More critically, the transfer of actinides from the primary site of incorporation (wound site for injuries/lung for inhalation) to the systemic circulation (input function into blood compartment), which is crucial information for the proper modelling of the chelation processes, is not known. Trying to derive this information using generic models with reference parameter values, i.e., not specific for the individual case under study, will merely introduce a perturbing bias in the analysis. The many unknowns and uncertainty sources associated with human incorporation cases make it difficult if not impossible to identify the chelation sites and estimate the values of the rate constants.

An alternative to using human data is the use of experimental data from controlled animal studies, for which all boundary conditions are known, thus leaving the definition of the sites of chelation and chelation rate constants as the only real unknown variables of the system. In the present work, models for describing the mechanism of the DTPA decorporation of Am in contaminated rats have been developed based mainly on results from rat studies conducted in the Laboratory of Radio Toxicology (LRT) of the French Commission of Atomic Energy and Alternative Energies (Commissariat à l'Energie Atomique et aux Energies Alternatives, CEA, France). Part of these data related to rats contaminated with Am-citrate with or without treatment through a single intravenous injection of different quantities of DTPA at different times before or after contamination (prophylactic and delayed treatments) was published in Grémy et al. (2016). The present work focuses exclusively on data from delayed treatment studies, in which DTPA was administered at Day 1 after Am contamination or later, i.e., at a time when Am content in blood is negligible with respect the early post-contamination phase. This set of data thus enabled us to focus our attention on the chelation mechanisms for Am not in blood, i.e., on the long-term effects of DTPA decorporation studies.

Adopting the CONRAD approach (Breustedt et al. 2009), simplified systemic models for the kinetics of Am-citrate and DTPA in rats were developed. In addition to the assumption that chelation can occur only in the ECF, hepatocytes were also considered a possible chelation site to account for the reduction in liver burden and the enhancement of faecal excretion. The aim is to transfer the gained knowledge to the human model and apply this knowledge to the existing human incorporation cases.

2. Materials and methods

2.1. Data

The models were fit to literature data and archive data (unpublished) provided by CEA/LRT in the framework of the EURADOS collaboration. An outline of the type of data and of the relative studies is given below. The whole set of data is made available as supplementary material.

The Am studies at CEA/LRT were all performed under the same experimental conditions, administering 9.42 kBq Am-citrate to each rat. The precise description of the experimental setup of these studies and additional details on the used solutions, animal housing setup, contamination procedure, chelation treatment and collection and measurement of urine, faeces and tissue samples are the same as those documented in Grémy et al. (2016). An outline of the type of data and of the relative studies is given below.

2.1.1. Americium citrate (controls)

- Uptake in and clearance from blood (Table A1): data from CEA/LRT studies and Turner and Taylor (1968). Data are expressed as the percentage of the injected activity (% IA; mean ± SD).
- Uptake in liver and the skeleton: data from the studies conducted at CEA/LRT. Organ retention on Day 14 was 7.06 ± 0.99% for the liver and 46 ± 3% for the skeleton. Data are expressed as the percentage of the injected activity (% IA; mean ± SD; n=4).
- Am excretion in urine and faeces (Tables A2 and A3): data from the studies conducted at CEA/LRT; data are given as 24 hours cumulative excretion, expressed as the percentage of the injected activity (% IA; mean ± SD).

2.1.2.DTPA

Data on the kinetics of DTPA were obtained from unpublished studies conducted at CEA/LRT. Pu-DTPA chelates were prepared *in vitro* at a concentration equivalent to a DTPA dose of 30 µmol·kg^{-1} and were administered intravenously in male Sprague Dawley rats (12.2 kBq in 200 µl).

- Uptake in and clearance from blood: data from the CEA/LRT studies (Table A4). Data are expressed as the percentage of the injected activity (% IA). A standard deviation of 30% was assumed for the Pu-DTPA data. This value was found to be a typical standard deviation for plasma clearance in other similar experiments conducted at CEA/LRT.
- DTPA elimination in urine: data from the CEA/LRT studies (Table A5). Data are presented as cumulative excretion expressed as the percentage of the injected activity (% IA). The standard deviation was set equal to the measurement error, or to 3 % of the measured value (whichever the highest).
- DTPA elimination in faeces: Although the experimental evidence on DTPA in humans and animals shows that more than 99% is excreted very rapidly in urine, tiny amounts of injected [^{14}C]DTPA were still detected in the bile of rats (0.12% at 24 h) (Bhattacharyya and Peterson 1979), which was associated with faecal excretion.

Additional data on the kinetics of DTPA complexes (^{99m}Tc-DTPA and ^{153}Gd-(DTPA)$^{2-}$) in blood and urine, presented by Wedeking et al. (1990), were used to check the model predictions. A special feature of this dataset is that the blood clearance was studied in detail in the first few minutes after administration. The uncertainty of the blood data corresponds to the 95% confidence interval for each data point, as given in the original reference. The urinary excretion data (Table 2 in Wedeking et al. (1990)) are given as (% IA; mean ± SD; n=6).

2.1.3.DTPA decorporation studies

Data from three decorporation studies conducted at CEA/LRT were used. In these experiments, rats were administered 300 µmol·DTPA kg^{-1} body weight on Day 1 (Experiment A), 3 (Experiment B) and 7 (Experiment C) after contamination with 9.42 kBq Am-citrate.

- Uptake in liver and the skeleton (Table A6: data from the studies conducted at CEA/LRT; Data for organ retention on Day 14 are expressed as the mean percentage of the injected activity (% IA; mean ± SD; n=4).
- Am excretion in urine and faeces: (Tables A7 and A8: data from the studies conducted at CEA/LRT; Data are given as 24 hours cumulative excretion, expressed as the percentage of the injected activity (% IA; mean ± SD; n=4).

2.2. Chelation Modelling and Model Assumptions

In biokinetic models used in radiation protection, human organs and tissues are generally simplified as separate compartments, and the translocations of materials between the organs and tissues are described by transfer rates. These biokinetic models are used to describe the time-dependent activity of a given incorporated radionuclide in the biological compartments.

After chelation therapy, the model should describe simultaneously the biokinetics not of one but of three forms: the incorporated Am, the DTPA and the Am-DTPA chelate. The CONRAD approach relies on the simultaneous use of three separate model structures to describe the biokinetic behaviour of the three available forms (Breustedt et al. 2009). As the kinetics of the Am-DTPA chelate are assumed to be the same as the kinetics of DTPA, the model structures of these two forms are identical. The three structures are combined together assuming that the *in vivo* chelation of Am by DTPA is proportional to the concentrations of both DTPA and actinide, mathematically described as a second-order kinetics process.

Assuming chelation between Am in a given compartment j of the Am model structure and DTPA in a given compartment i of the DTPA model structure, the formation of Am-DTPA chelates in compartment i can be written as

$$\frac{dz_i}{dt} = -\sum_{h=1}^{m} k_{hi} z_i + \sum_{h=1}^{m} k_{ih} z_h + \sum_{j=1}^{n} kR_{ij} \cdot f(x_j, y_i) = \sum_{h=1}^{m} (k_{ih} z_h - k_{hi} z_i) + \sum_{j=1}^{n} kR_{ij} \cdot f(x_j, y_i)$$

with

$$f(x_j, y_i) = x_j \cdot y_i$$

and

- x_j is the time-dependent content of the j^{th} compartment in the Am model [in moles]
- y_i is the time-dependent content of the i^{th} compartment in the Am model [in moles]
- z_h is the time-dependent content of the h^{th} compartment in the Am model [in moles]

The sum index h runs from 1 to m (number of compartments in the systemic model of DTPA, the same as in the model of Am-DTPA), k_{hi} is the transfer coefficient describing passage from compartment i to compartment h of the DTPA model (same as for Am-DTPA) and the last sum is over all compartments x_j of the Am model where chelation with DTPA in compartment i can occur.

Consequently, the equation for DTPA (y_i) in compartment i is given by

$$\frac{dy_i}{dt} = -\sum_{h=1}^{m} k_{hi} y_i + \sum_{h=1}^{m} k_{ih} y_h - \sum_{j=1}^{n} kR_{ij} \cdot f(x_j, y_i) = \sum_{h=1}^{m} (k_{ih} y_h - k_{hi} y_i) - \sum_{j=1}^{n} kR_{ij} \cdot f(x_j, y_i)$$

and the equation for Am in compartment j (x_j) is given by

$$\frac{dx_j}{dt} = -\sum_{l=1}^{n} k_{lj}^{Am} x_j + \sum_{l=1}^{n} k_{jl}^{Am} x_l - \sum_{i=1}^{m} kR_{ij} \cdot f(x_j, y_i)$$
$$= \sum_{l=1}^{n} (k_{jl}^{Am} x_l - k_{lj}^{Am} x_j) - \sum_{i=1}^{m} kR_{ij} \cdot f(x_j, y_i)$$

where the sum index l runs from 1 to n (the number of compartments in the systemic model of Am), k_{hj}^{Am} is the transfer coefficient describing passage from compartment j to compartment h of the Am model and the last sum is over all compartments y_i of the DTPA model where the chelation of Am with DTPA in compartment i can occur.

As one DTPA molecule can chelate one Am ion, the Am and DTPA entities in a given chelation site both disappear with the same rate $kR_{ij} \cdot x_j \cdot y_i$, proportional to the rate constant kR_{ij} and to the molar contents of Am and DTPA in the sites where chelation occurs. The Am-DTPA chelate appears in the corresponding site of DTPA and with the same chelation rate.

2.3. Model Implementation and Fitting

The model structures and the underlying equations were implemented using SAAM II software (©The Epsilon Group, Charlottesville, Virginia, USA). SAAM II is a software package that is applied to build models, run simulations and analyse results. The values of the adjustable parameters were estimated using the fitting tools and algorithms available in the SAAM II software package. The objective function to be minimized is defined in the SAAM software as the extended least-squares maximum likelihood function. It depends among others on the residuals, i.e., the differences between the model predictions and the experimental data, and on the variance associated to them (Barrett et al., 1998). The variance model was chosen, in order to reflect different levels of reliability of the different types of data available.

Other indicators of the goodness of fit used in addition to the convergence criterion were:

- The coefficient of variation of the parameters, as calculated by the software, that corresponds to 1 SD and is expressed as a fraction of the parameter estimate;
- The correlation coefficients, that was used to identify any correlations between the parameters and therefore the possibility of simplifying the structure of the model, in order to pursue the principle of model parsimony;
- The Akaike Information Criterion [AIC] and the Bayesian Information Criterion [BIC], which were used to compare competing structures (again in compliance with the parsimony principle).

A fit was therefore considered successful based on the combination of these different indicators.

First, the model structures had to be defined, and all the model parameters were considered to be "adjustable". They were estimated separately for the Am- and DTPA-models using the respective data (see Material and Methods section, Tables in the supplementary material). Thereafter, the calculated transfer coefficients were kept fixed, while the only unknown parameters, the chelation rate constants kR_{ij}, were fitted simultaneously to the overall dataset of all decorporation experiments (A, B and C). For the model analysis, the cumulative activity over the entire measurement period was calculated by the summation of the daily excreted activities.

The identification of the chelation sites and the chelation rate constants are thus the only unknown variables of the system.

3. Results

3.1. DTPA Biokinetic Model for Rats

The model structure for DTPA kinetics in rats is based on the one previously developed by Breustedt et al. (2009) starting from human data presented by Stather et al. (1983). Based on the information that 0.12% of the injected [^{14}C]DTPA was excreted into bile by 24 h after DTPA administration, the ability of DTPA to enter hepatocytes to a small extent prior to its biliary/faecal elimination (Stevens et al. 1978; Bhattacharyya 1978a; Bhattacharyya and Peterson 1979; Ballou and Hess 1972) can be assumed. This is in accordance with the fact that delayed DTPA treatments enhanced biliary/faecal clearance of Pu/Am in rats (Bhattacharyya et al. 1978a; Bhattacharyya and Peterson 1979; Ballou and Hess 1972), dogs (Stevens et al. 1978; Grémy et al. 2016), pigs (Smith et al. 1961) and humans (Norwood 1960; Roedler et al. 1989; James et al. 2007; Grémy et al. 2021; Grémy et al. 2022). To take this into account, the structure was modified by adding a compartment to represent hepatocytes and a new path to faecal loss to reproduce the excretion of DTPA chelates in faeces (**Figure 1**).

The parameter values of the modified model were estimated based on the CEA/LRT data on Pu-DTPA kinetics in rats (s. 2.1.2) and are shown in Table 1. In line with the approach pursued by the CONRAD project and with the available data, it is assumed that the biokinetic behaviour of DTPA complexes is independent of the ligand due to the comparatively large dimension of the DTPA molecule. Furthermore, no dependence is assumed on the ionic charge.

The identification of the two compartments representing the ECF as *interstitial fluids* and *lymph*, made in (Breustedt et al. 2009), merely reflects a physiological assumption and cannot be substantiated by experimental data. For this reason, these compartments are indicated here as "ECF-Fast exchange" and “ECF-Slow exchange" in **Figure 1**.

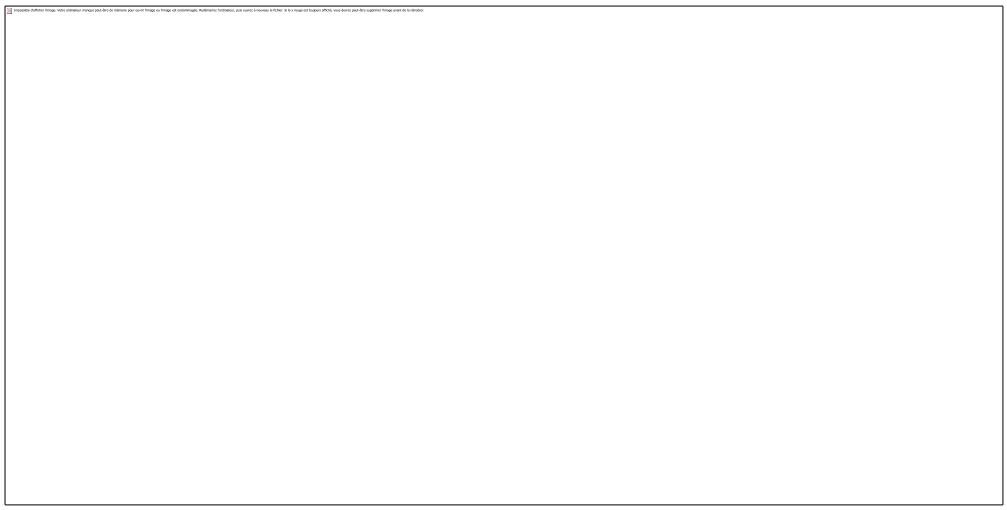

Figure 1*: Compartmental model of DTPA kinetics in rats. ECF stands for extracellular fluids. The shaded area corresponds to the circulating DTPA.*

Table 1: Parameters of the model in Figure 1

Pathway	Transfer rate value (d^{-1})
Urinary Bladder → Urine	$(1.5\pm0.4)\cdot10^{2}$
Blood → Urinary Bladder	$(2.85\pm0.06)\cdot10^{2}$
ECF-Fast exchange → Blood	$(3.1\pm0.2)\cdot10^{2}$
ECF-Slow exchange → Blood	$(8.0\pm0.5)\cdot10^{-1}$
Blood → ECF-Fast exchange	$(1.15\pm0.05)\cdot10^{3}$
ECF-Fast exchange → ECF-Slow exchange	$(1.20\pm0.08)\cdot10^{1}$
ECF-Fast exchange → Hepatocytes	$(9.7\pm1.0)\cdot10^{-2}$
Hepatocytes → Faeces	$(9.48\pm0.22)\cdot10^{-1}$

Figure 2 and **Figure 3** show the experimental data of the CEA/LRT studies and the corresponding DTPA model predictions for urine and plasma, respectively. For comparison, the data from Wedeking et al. (1990), not used for the model fitting, are also shown.

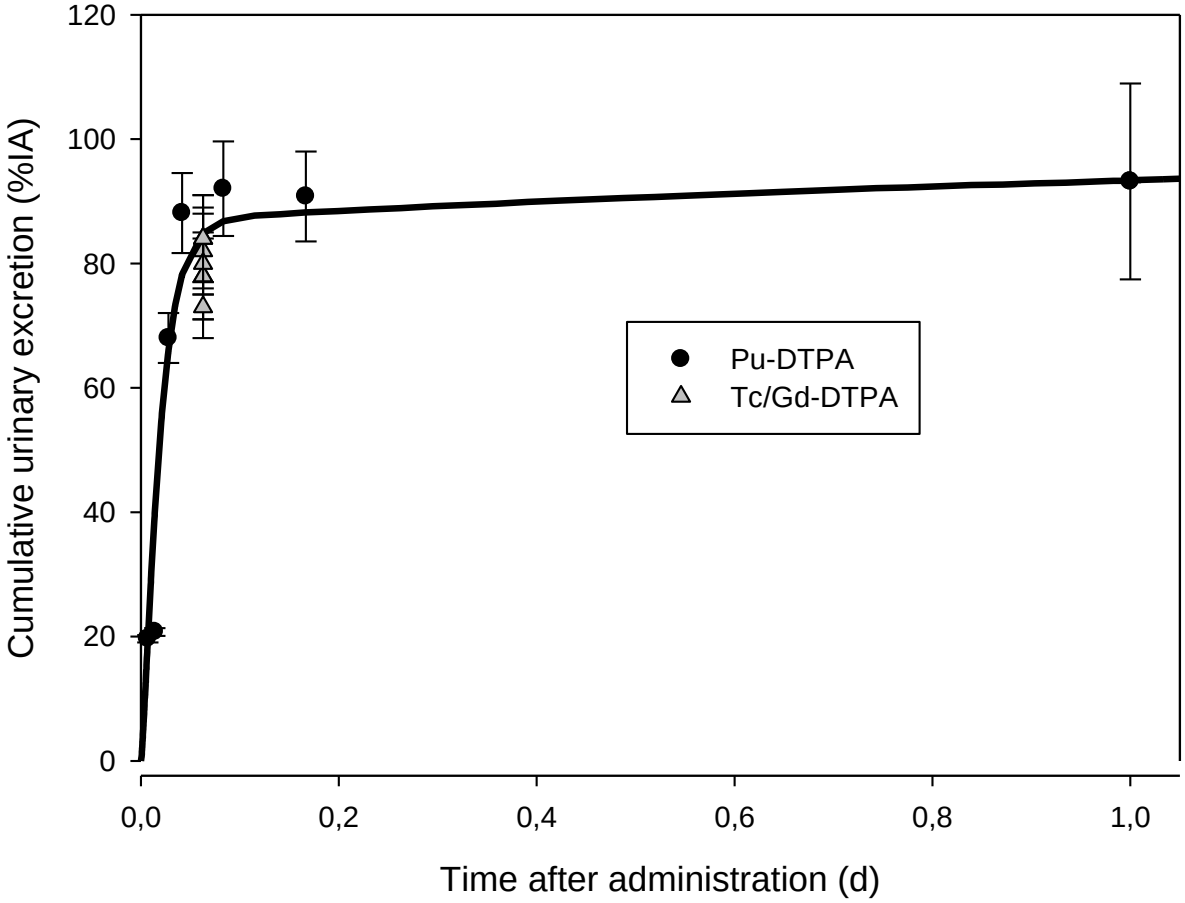

Figure 2 *Cumulative urinary excretion of DTPA in rats. Solid line: model prediction; black dots: Pu-DTPA, provided by CEA/LRT; grey triangles: Tc/Gd-DTPA, from Wedeking et al. (1990)*

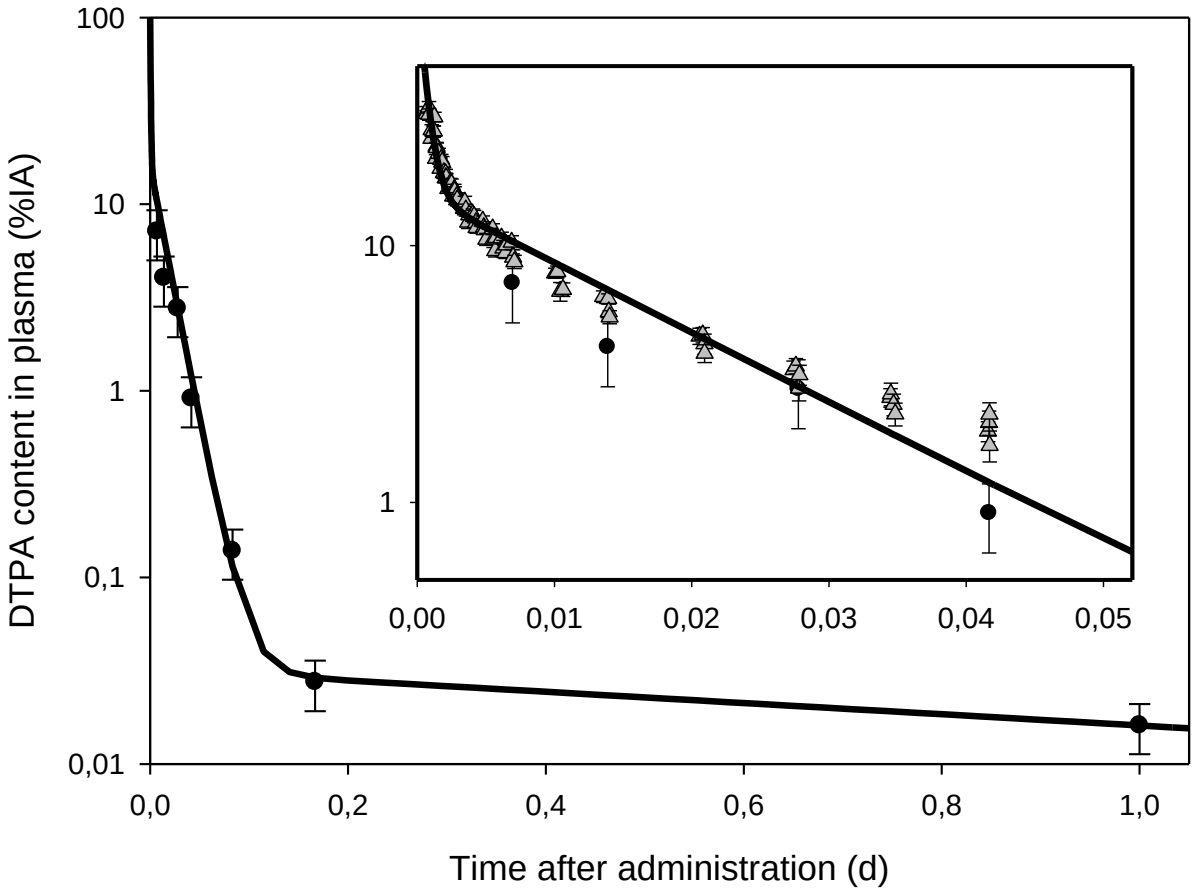

Figure 3 *Clearance of DTPA in blood of rats. Solid line: model prediction; black dots: Pu-DTPA, provided by CEA/LRT; grey triangles: Tc/Gd-DTPA, from Wedeking et al. (1990)*

3.2. Americium Rat Model

The model structure for Am biokinetics in rats, shown in **Figure 4**, was developed based on the knowledge that Am preferably accumulates in the liver and skeleton. Am in blood plasma is divided into two compartments (Blood1 and Blood2) to consider short and long retention of Am in plasma. Both plasma compartments exchange material with identified organs and tissues: the skeleton, liver and kidney. Other organs and tissues to which Am can be transferred were pooled into two generic soft tissue compartments (ST0 and ST1). Faecal excretion is channelled directly from the liver (Liver 2).

The overall model structure was developed using the complete available dataset of the control rats (2.1.1). Table 2 shows the parameter values corresponding to the best fit to the available data. These were then kept fixed in the next step of the analysis of the chelation study data.

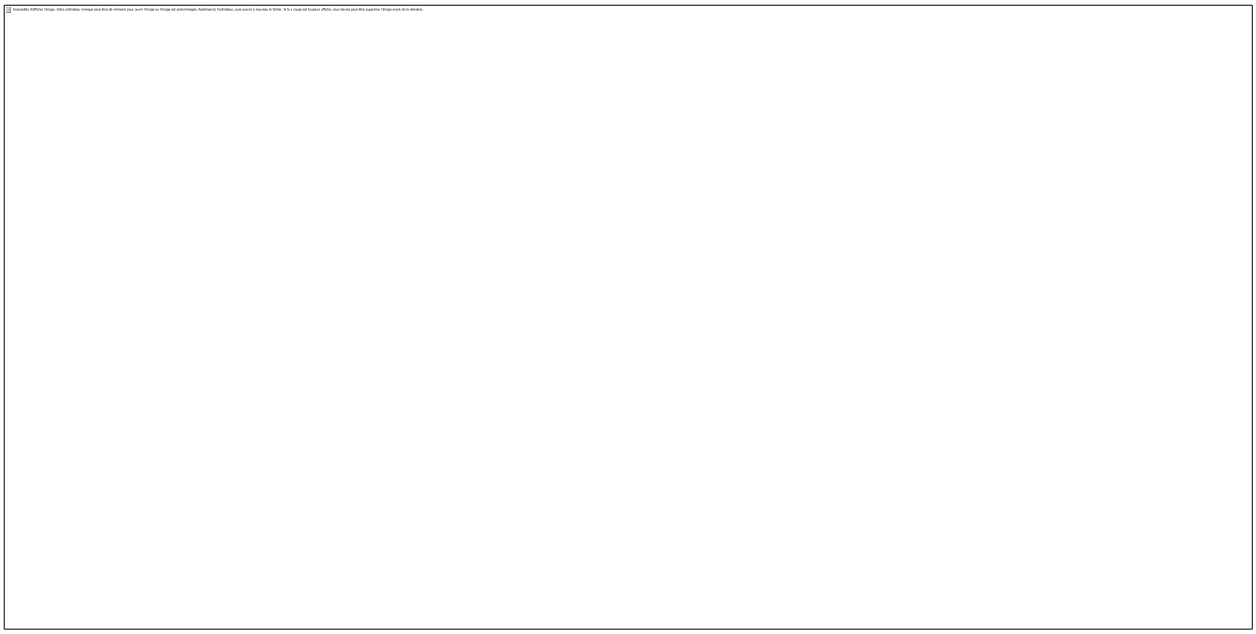

Figure 4 *Compartmental model of Am kinetics in rats*

Table 2: Parameters of the model in Figure 4

Pathway	Transfer rate value (d^{-1})
Blood1 -> Liver1	$(7.1\pm0.2)\cdot10^{4}$
Blood2 -> Blood1	(5.4 ± 0.6)
Blood1 -> Blood2	$(5.4\pm0.3)\cdot10^{4}$
Blood2 -> Liver1	$(6.7\pm0.5)\cdot10^{-1}$
Liver1 -> Blood1	$(7.0\pm0.9)\cdot10^{-2}$
Liver1 -> Liver2	$(1.35\pm0.05)\cdot10^{-1}$
Liver2 -> Faeces	$(5.1\pm0.2)\cdot10^{-1}$
Blood1 -> ST0	$(2.5\pm0.2)\cdot10^{-2}$
Blood2 -> ST0	$(6.0\pm0.2)\cdot10^{1}$
ST0 -> Blood1	$(3.6\pm5.3)\cdot10^{-3}$
ST0 -> Blood2	(18.1 ± 1.8)
ST0 -> ST1	(9.4 ± 1.0)
ST1 -> Blood2	(2.81 ± 0.02)
Blood1 -> Skeleton1	$(1.7\pm1.4)\cdot10^{-1}$
Blood2 -> Skeleton1	$(4.26\pm0.02)\cdot10^{1}$
Skeleton1 -> Blood1	$(2.18\pm0.11)\cdot10^{-1}$
Skeleton1 -> Skeleton2	(1.1 ± 0.2)
Kidney -> Blood1	$(2.93\pm0.17)\cdot10^{-2}$
Kidney -> Blood2	$(6.3\pm0.4)\cdot10^{-2}$

Blood1 -> Kidney	$(3.6\pm0.4)\cdot10^{4}$
Blood1 -> Urinary Path	$(1.73\pm0.17)\cdot10^{4}$
Blood2 -> Urinary Path	$(5\pm3)\cdot10^{-1}$
Urinary Path -> Urine	(2.32±0.15)

Figure 5 shows the model predictions compared to the available data for Am urine excretion (black dots and solid line) and Am faecal excretion (grey triangles and dashed line) in control rats. Figure S1 shows the plasma clearance data and the corresponding model predictions.

3.3. Assumptions for chelation

The challenging part of the CONRAD approach (Breustedt et al. 2009) is the definition of the sites where chelation occurs, which corresponds to the selection of the appropriate combinations of the interacting compartments. The proposed model for DTPA consists of the compartments "Blood", "ECF-Slow exchange", "ECF-Fast exchange" and "Hepatocytes" in addition to the excretion paths. The most straightforward assumption is that DTPA in the ECF compartments chelates Am in the blood compartments of the Am model and DTPA in the hepatocytes chelates Am in the liver compartments. Furthermore, the compartments that receive direct inflow from blood, i.e., liver1, skeleton1, kidney and ST0, are assumed to be partly associated with the ECF circulating in the corresponding tissue, so that part of the Am contained there is also available for chelation with DTPA in the ECF compartments. Therefore, all possible combinations of these compartments with DTPA in "Blood", "ECF-Slow exchange" and "ECF-Fast exchange" were tested.

Since chelation dynamics and efficiency depend on the surrounding environment, such as the presence of other endogenous ligands or competing metals, different chelation rate constants were considered for each combination of the relevant compartments.

Based on the results of the model fits, the following combinations were found to be sufficient to describe the complete set of data:

- Am in "Kidney" is chelated with DTPA from the "Blood" compartment, but not with DTPA from the "ECF-Slow exchange" and "ECF-Fast exchange" compartments.
- Am in the "Liver1" compartment is chelated with DTPA from the "ECF-Slow exchange" and "Hepatocytes" compartments, but not with DTPA from the compartments "Blood" and "ECF-Fast exchange".

Table 3 shows the values of the chelation rate constants as obtained in the model fits. For kR2 it was not possible to find a common value which was able to simultaneously describe the complete set of data. So the fits were performed with three different parameter values of kR2, one for each experiment (as indicated in the last column of Table 3).

Table 3: Values of the chelation rate constants

Chelation rate constant	Combined model compartments	Value ($d^{-1}\cdot mol^{-1}$)	Experiment
kR1	$DTPA_{ECF\text{-}Slow\ exchange}$ and Am_{Liver1}	$(7.2\pm0.08)\ 10^{-2}$	A and B and C
kR2	$DTPA_{Blood}$ and Am_{Kidney}	2.02±0.06	A
		2.43±0.01	B

		3.34±0.11	C
kR3	$DTPA_{hep}$ and Am_{Liver1}	16.04±0.31	A and B and C

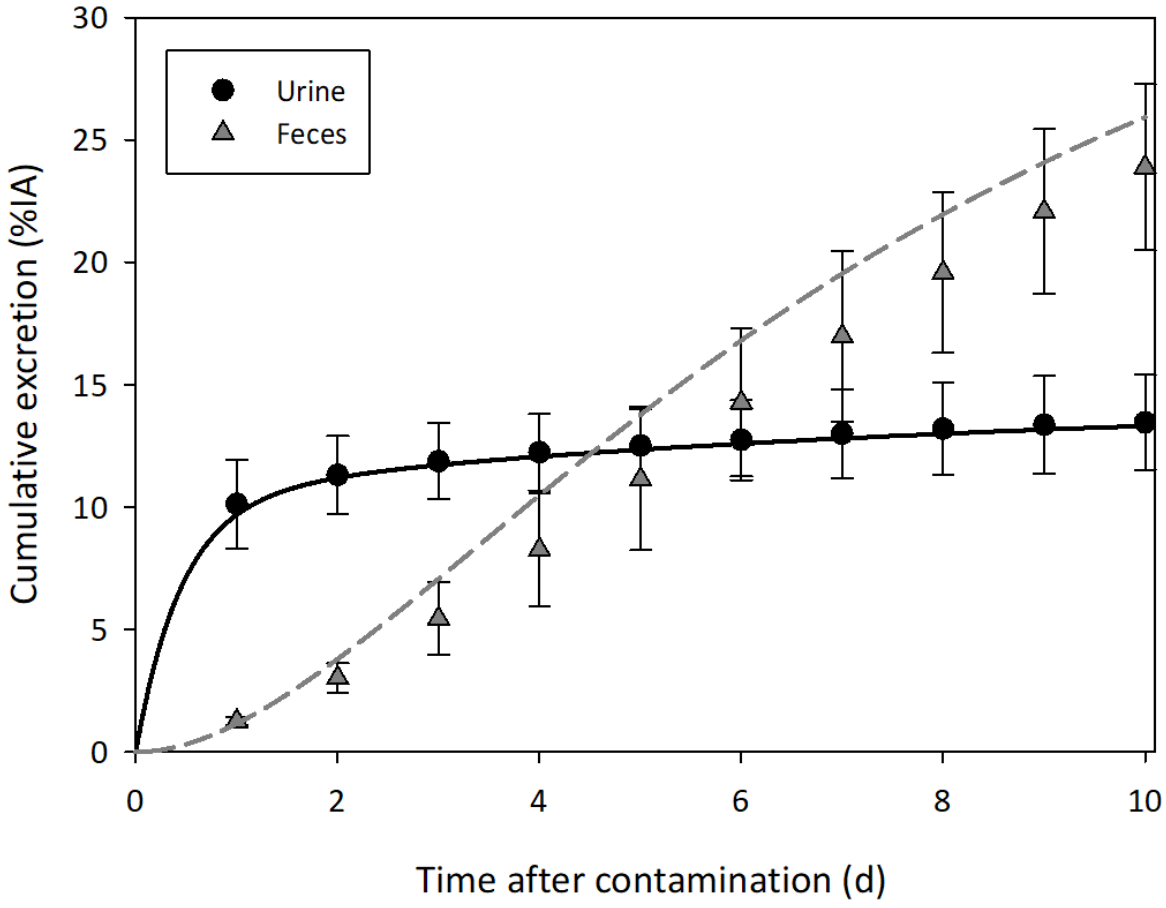

Figure 5 *Comparison of model prediction and data for the cumulative excretion of Am in control rats. Black solid line and black dots: urine. Grey dashed line and grey triangles: faeces.*

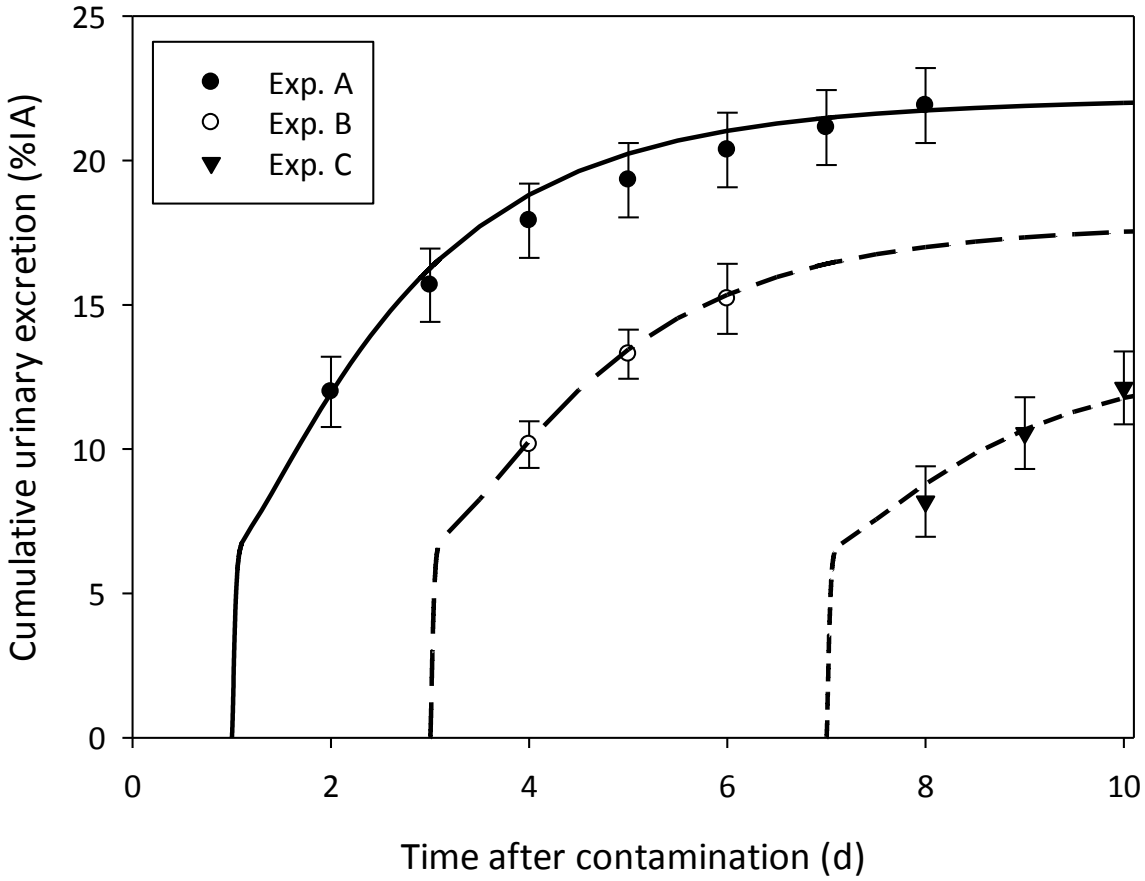

Figure 6 *Comparison of model prediction and data for cumulative urinary excretion in chelation studies. Experiment A (300 µmol·kg^{-1} DTPA on Day 1): black solid line and black dots; Experiment B (300 µmol·kg^{-1} DTPA on Day 3): black dashed line and empty dots; Experiment C (300 µmol·kg^{-1} DTPA on Day 7): black dashed line and black triangles.*

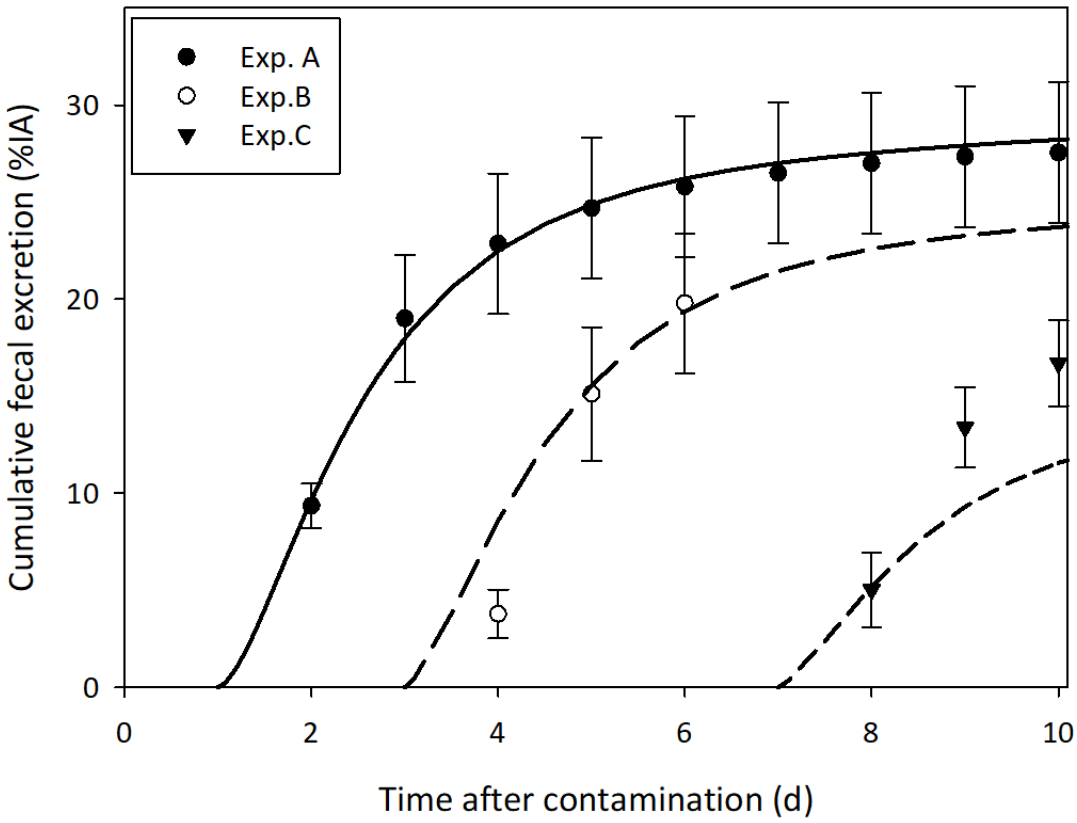

Figure 7 *Comparison of model prediction and data for the cumulative faecal excretion in the chelation studies. Experiment A (300 µmol·kg^{-1} DTPA on Day 1): black solid line and black dots; Experiment B (300 µmol·kg^{-1} DTPA on Day 3): black dashed line and empty dots; Experiment C (300 µmol·kg^{-1} DTPA on Day 7): black dashed line and black triangles.*

3.4. Excretion

In Figures 6 and 7, model predictions of the urinary and faecal excretion in the DTPA decorporation studies (Experiments A, B, C) are given, respectively. Data and model predictions are presented as cumulative excretion expressed as the percentage of the injected activity (% IA). Data were calculated as the mean values of *4* rats (mean ± SD; *Table A7, Table A8*).

The curves correspond to the results that fulfilled the goodness-of-fit criteria described in section 2.3. In general, a good agreement between model prediction and data can be seen for all studies. The model prediction curve for faecal excretion for control rats systematically overestimates the experimental data; however, it is still within the experimental uncertainties. The curve of the faecal excretion for Experiment C cannot describe the data.

The model proved able to describe the general effect observed during the experiments, with the enhancement of urinary excretion inversely depending on the delay of DTPA administration after Am contamination.

3.5. Organ retention

Table 4 and 5 show the effect of DTPA treatment on Am retention in the liver and skeleton compared to untreated controls. The data are presented as the DTPA-induced reduction in Am uptake in tissues and are expressed as the mean percentage reduction relative to the corresponding untreated group (%; mean ± SD).

The agreement between the model and the data is in general remarkable for the liver regardless of the time of DTPA administration. On the contrary, reduction in skeleton cannot be reproduced.

Table 4: Comparison of model prediction and experimental data on the reduction of Am uptake in rat liver after delayed DTPA treatment

	time of measurement (d)	time of DTPA treatment after contamination (d)	data (%; mean ± SD)	model (%)
Experiment A	14	1	85±28	81
Experiment B	14	3	84±18	84
Experiment C	14	7	82±20	85

Table 5: Comparison of model prediction and experimental data on the reduction of Am uptake in rat skeleton after delayed DTPA treatment

	time of measurement (d)	time of DTPA treatment after contamination (d)	data (%; mean ± SD)	model (%)
Experiment A	14	1	40±3	18
Experiment B	14	3	35±5	15
Experiment C	14	7	24±3	9

4. Discussion

In this study, a system of models for DTPA-induced decorporation of Am was developed based on excretion and tissue data from animal studies conducted at CEA/LRT as well as additional relevant data taken from the literature. The simplified substructures, of which this system of models is composed, describe the three available forms: the incorporated Am-citrate, the DTPA and the Am-DTPA chelate.

A recent publication (Miller et al. 2019) presented a model of the systemic biokinetics of Am in rats starting from a comprehensive dataset including the pelt, liver, skeleton, lung, GI-tract, spleen, kidneys, muscle, ST and gonads. This model is based on pharmacokinetic considerations. The model parameters were assessed from the physiological knowledge of the vascular flows to the tissues and of the volumes of the extracellular fluids associated with each tissue. Extrapolation to early times was made with small uncertainties by using pharmacokinetic front-end modelling.

Figure 2 and Figure 3 show that the data of Wedeking et al. (1990) on the kinetics of DTPA complexes, which were not used for the model fit, can also be described by the model curves. This suggests the validity of the assumption that the biokinetics of DTPA is independent of the type of chelated molecule and the ionic charge, and that the proposed structure, although simplifying much more complex processes, can successfully describe all available experimental data.

The fact that the data at our disposal originate from DTPA decorporation studies with DTPA administration at least one day after contamination proved to be the major challenge for the definition of the sites of chelation and the mechanism of the chelation process itself, since at day 1 after contamination only about 0.1% of the injected americium is present in blood. However, this enabled to focus the analysis on the long-term effects of DTPA decorporation studies. The parameter values shown in Table 3 represent the results of the model fits and the minimal set of chelation rate constants (kR) needed to describe the available data. The results are satisfactory in terms of model parsimony considering that only three chelation sites are sufficient to successfully reproduce all the studies. However, it was not possible to obtain an unique value of kR2, which is the rate constant describing the chelation of Am in the kidneys with DTPA in blood. It was possible to obtain a satisfactory fit only considering different values of kR2 for each of the three experiments, with kR2 increasing with increasing delay of DTPA tratment. This proves that the simple assumptions of second-order kinetics made in the CONRAD approach are not always sufficient to provide a globally valid set of values for the chelation rate constants. It is important to consider that the assumptions behind the model structures are simplifications of complex processes. Nonconstant kR values indicate the possibility that more complex kinetics are at stake, which, however, cannot be better modelled with available information.

According to the results, the compartment “kidneys” in the Am model is identified as one of the sites where chelation with DTPA occurs. Considering that blood makes up approximately 26.5% of the total kidney mass, according to ICRP Publication 133 (Bolch et al. 2016), it seems reasonable to assume that the Am activity present in the “Kidney” compartment can be partly associated with blood and can thus be seen as a possible site of chelation with DTPA in blood. Similarly, the activity in the “Liver1” compartment can be associated with the ECF and therefore can be seen as a possible site of chelation with DTPA in the “Slow exchange” compartment of the ECF, as has been done before e.g. in Breustedt et al. (2019). These chelates are eliminated in the urine.

In general, it is assumed that once bound in the retention organs, the actinide is no longer physically available to the chelating agent until released by natural recycling into ECF due to loss from soft tissues. However, even though the penetration of the DTPA molecule into the cell is not an obvious assumption due to its physico-chemical properties, according to several authors, DTPA might be present in small amounts in the hepatocytes and thus be available for chelation of Am prior to bile/faeces elimination. Stevens et al. showed that as soon as 2 h after [^{14}C]DTPA injection into rats, the ratio of the concentration of DTPA in the liver to that in plasma was greater than 1, reaching a maximum of 4 at 4 h, and this ratio was still greater than 3 at 48 h (Stevens et al. 1978). This indicates that DTPA molecules can penetrate liver cells, including hepatocytes, where they are retained. In addition, [^{14}C]DTPA was detected in the bile of injected rats (0,12% at 24 h), thus showing the ability of DTPA to enter hepatocytes to a small extent prior to its biliary/faecal elimination (Stevens et al. 1978; Bhattacharyya 1978a; Bhattacharyya and Peterson 1979; Ballou and Hess 1972). In rats, 80 to 90% of the Pu present in the bile is in the form of Pu-DTPA chelate (Bhattacharyya and Peterson 1979). The only elimination pathway for the An-DTPA chelates formed inside hepatocytes is the biliary/faecal route, which is evidenced by an enhancement of faecal excretion, as shown in the data, and can be reproduced by the proposed model (see Table A8, **Figure**

484 **7Erreur ! Source du renvoi introuvable.Erreur ! Source du renvoi introuvable.**). The agreement for
485 the faecal excretion is less satisfactory than for urine. Faecal excretion data, as well skeletal
486 retention data, were considered to be associated with substantial uncertainties and given a lower
487 weighting in the fit process.

488 The available data clearly indicate the effect of delayed DTPA treatment on Pu/Am retention in
489 bones as well. One hypothesis could be that a part of bone Am remains available for chelation: a
490 substantial reduction in skeletal burden in a DTPA-treated human case was observed to occur in
491 trabecular bone (James et al. 2007). Taylor (1989) showed that a Pu/Am fraction is still associated
492 with bone surfaces for at least 7 days after rat contamination. However, tests with the proposed
493 model involving direct chelation in the skeletal compartments were unsuccessful. Evidently, the
494 systemic chelation assumed in the proposed model is not sufficient to reproduce the observed
495 reduced uptake and retention in the skeleton. Additionally, in the fitting process it was not possible
496 to find a value for the rate constants describing chelation in the skeletal compartments greater than
497 zero. Possible reasons for this may be the large uncertainties in the available data. Activity in the
498 skeleton was indeed estimated from measurements in two femurs by scaling the result to the whole
499 skeleton under the assumption that the two femurs represent 10% of the total bone (Grémy et al.
500 2016). However, this value may show significant between subjects variations, so these results were
501 considered less reliable than the others in the fitting process and a large variance was associated to
502 this dataset. Additional work is needed to correctly reproduce the long-term retention of Am in the
503 skeleton. This has only a negligible impact on the description and interpretation of the excretion
504 data. Nevertheless, the correct reproduction of the skeletal burden would be important for the
505 calculation of the dose, especially at later times.

506

507 **5. Conclusions**

508 In the presented work, an approach for describing the unperturbed biokinetics of Am and DTPA, the
509 chelation process and the behaviour of the Am-DTPA compound with a single model system has
510 been applied to rat data. For this, models to describe the biokinetic behaviour of unperturbed Am
511 and DTPA in rats were developed, which were then combined into a model system by a suitable
512 mathematical description of the chelation mechanism as a second-order process. The proposed
513 model system is able to describe the vast majority of excretion and tissue data from animal studies
514 for DTPA-induced Am decorporation and for pure Am biokinetics conducted by CEA/LRT, with the
515 only exception of skeleton in all experiments. Long-term effects of chelation of DTPA following
516 treatment at Day 1 post contamination with Am or later can be described assuming three possible
517 sites of chelation. For chelation in kidney the value of the chelation rate coefficient depends on the
518 delay of DTPA treatment. Considering the scarcity of the available data and the uncertainties
519 inherent in this kind of study, further experimental work is needed to reach a deeper understanding
520 of the interpretation of this phenomenon.

521 The compartmental structure presented in this paper and developed from the CONRAD approach
522 identified three chelation sites that allow to describe the long-term effects of DTPA treatment on the
523 kinetics of incorporated Am with regard to excretion and reduced uptake in the liver. The analysis
524 presented has been affected by limitations on the available data and the inability to find a valid set
525 of common parameter values for all experiments, indicating that the simplifications inherent in the
526 basic assumptions of the model fail to account for the complexity of the processes involved.

Nevertheless, the obtained results can contribute to improve the interpretation of biological data from DTPA-treated contamination cases and the modelling of Am decorporation by protracted DTPA treatment, and help to estimate the incorporated activity and to assess the benefit of the therapy in terms of the averted dose. Further experimental research is still needed to reach a better understanding of the physiological processes and for a future translation of the findings to human models.

6. Statements and Declarations:

Conflicts of interest: The authors declare that they have no conflicts of interest.

Financial interests: The authors declare they have no financial interests.

Funding: The authors did not receive support from any organization for the submitted work.

Data availability: Data are available in the text and additionally as supplementary information.

References

Reference list

Bailey BR, Eckerman KF, Townsend LW (2003) An analysis of a puncture wound case with medical intervention. Radiat Prot Dosim 105:509–12. doi: 10.1093/oxfordjournals.rpd.a006293. PMID: 14527019

Ballou, JE, Hess, JO (1972) Biliary Plutonium Excretion in the Rat, Health Phys 22(4): 369-372. https://doi.org/10.1097/00004032-197204000-00008

Barrett PH, Bell BM, Cobelli C, Golde H, Schumitzky A, Vicini P, Foster DM (1998) SAAM II: Simulation, analysis and modeling software of tracer and pharmacokinetic studies. Metabolism 47:484–492. https://doi.org/10.1016/S0026-0495(98)90064-6

Bertelli L, Poudel D, Klumpp J, Waters T (2018) A method for tracking a case under chelation using urinary excretion measurements. In: 12th international conference on the health effects of incorporated radionuclides (HEIR conference); 8-11 October 2018; Fontenay-aux-Roses, France. Les Ulis, France; EDP Sciences; 2018:02005.

Bertelli L, Waters TL, Miller G, Gadd MS, Eaton MC, Guilmette RA (2010) Three plutonium chelation cases at Los Alamos National Laboratory. Health Phys 99:532–538. doi: 10.1097/hp.0b013e3181d18c61. PMID: 20838095.

Bhattacharyya MH, Breitenstein BD, Métivier H, Muggenburg BA, Stradling GN, Volf V, Gerber GB (Eds.) (1992) Guidebook for the treatment of accidental internal contamination of workers. Radiat. Prot. Dosim. 41(3). https://doi.org/10.1093/OXFORDJOURNALS.RPD.A081216

Bhattacharyya MH, Peterson DP (1979) Action of DTPA on Hepatic Plutonium: III. Evidence for a Direct Chelation Mechanism for DTPA-Induced Excretion of Monomeric Plutonium into Rat Bile. Radiat Res 80 (1): 108–115. https://doi.org/10.2307/3575119

563 Bhattacharyya MH, Peterson DP, Lindenbaum A Action of DTPA on hepatic plutonium I. (1978a)
564 Quantitation of the DTPA-induced biliary excretion of plutonium in the rat. Radiat Res 74:179–85.
565 https://doi.org/10.2307/3574768

566 Bhattacharyya MH, Peterson DP, Lindenbaum A (1978b) Action of DTPA on Hepatic Plutonium: II.
567 DTPA-Induced Removal of Monomeric Plutonium from Mouse Liver Parenchymal Cells. Radiat Res 76
568 (1): 180–186. https://doi.org/10.2307/3574768

569 Breustedt B, Avtandilashvili M, McComish SL, Tolmachev SY (2019) USTUR Case 0846: Modeling
570 Americium Biokinetics After Intensive Decorporation Therapy. Health Phys. Special issue. 2019.
571 117(2): 168-178. doi:10.1097/hp.0000000000000931

572 Breustedt B., Blanchardon E, Bérard P, Fritsch P, Giussani A, Lopez MA, Luciani A, Nosske D,
573 Piechowski J, Schimmelpfeng J, Sérandour AL (2009) Biokinetic modelling of DTPA decorporation
574 therapy: the CONRAD approach. Radiation Protection Dosimetry 134, 38-48. doi:
575 10.1093/rpd/ncp058. Epub 2009 Apr 7. PMID: 19351653

576 Carbaugh EH, Decker WA, Swint MJ (1989) Medical and health physics management of a plutonium
577 wound. Radiat Prot Dosim 26:345–349. https://doi.org/10.1093/oxfordjournals.rpd.a080428

578 Carson ER, Cobelli C, Finkelstein L (1983) The Mathematical Modeling of Metabolic and Endocrine
579 Sytems. Model Formulation, Identification and Validation. Wiley, New York.
580 https://doi.org/10.1016/0270-0255%2886%2990115-6

581 Catsch A (1968) Dekorporierung radioaktiver und stabiler Metallionen – Therapeutische Grundlagen.
582 Thiemig, München

583 Cohen N, Guilmette RA, Wrenn ME (1974) Chelation of 241Am from the liver and skeleton of the
584 adult baboon. Radiat Res 58:439–47. https://doi.org/10.2307/3573913

585 Davesne E, Blanchardon E, Peleau B, Correze P, Bohand S, Franck D (2016) Influence of DTPA
586 treatment on internal dose estimates. Health Phys 110:551–557. doi:
587 10.1097/HP.0000000000000487. PMID: 27115221.

588 Dumit S, Avtandilashvili M, Strom DJ, McComish SL, Tabatadze G, Tolmachev SY (2019a) Improved
589 Modeling of Plutonium-DTPA Decorporation Radiat Res (2019) 191 (2): 201–210. doi:
590 10.1667/RR15188.1

591 Dumit S, Avtandilashvili M, McComish SL, Strom DJ, Tabatadze G, Tolmachev SY. (2019b) Validation
592 of a system of models for plutonium decorporation therapy. Radiat and Environ Biophys 58(2):227-
593 235. https://doi.org/10.1007/s00411-018-00773-y

594 Dumit S, Bertelli L, Klumpp JA, Poudel D, Waters T. (2020a) Chelation modeling: the use of ad hoc
595 models and approaches to overcome a dose assessment challenge. Health Phys 118(2): 193-205. DOI:
596 10.1097/HP.0000000000001134

597 Dumit S, Miller G, Klumpp JA, Poudel D, Bertelli L, Waters T. (2020b) Development of a new chelation
598 model: bioassay data interpretation and dose assessment after plutonium intake via wound and
599 treatment with DTPA. Health Phys 119(6): 715-732. DOI: 10.1097/HP.0000000000001282

600 Dumit S, Miller G, Poudel D, Bertelli L, Klumpp JA. (2023) Chelation Model Validation: Modeling of a
601 plutonium-238 inhalation incident treated with DTPA at Los Alamos National Laboratory. Health
602 Phys 124(2): 113-124. DOI: 10.1097/HP.0000000000001647

603 Durbin PW, in: Morss LR, Edelstein NM, Fuger J, Katz JJ (Eds.), third ed. (2006) The Chemistry of the
604 Actinide and Transactinide Elements. Springer New York vol. 5, p. 332. https://doi.org/10.1007/978-
605 94-007-0211-0

606 Durbin PW, Kullgren B, Schmidt T (1997) Circulatory kinetics of intravenously injected 238Pu(IV)
607 citrate and 14C-CaNa3-DTPA in mice: comparison with rats, dog, and reference man. Health Phys
608 72:222–35. doi: 10.1097/00004032-199702000-00005. PMID: 9003707.

609 FDA (2015) FDA approves drugs to treat internal contamination from radioactive elements.
610 https://www.fda.gov/drugs/bioterrorism-and-drug-preparedness/fda-approves-drugs-treat-internal-
611 contamination-radioactive-elements. Last accessed 13.01.2023

612 Fisher DR (2000) Health Phys. 78 DECORPORATION: OFFICIALLY A WORD. Health Phys: The Radiation
613 Safety Journal 78(5):563-565. doi: 10.1097/00004032-200005000-00015

614 Fouillit M, Grillon G, Fritsch P, Rateau G, Pavé D, Delforge J, et al. (2004) Comparative tissue uptake
615 and cellular deposition of three different plutonium chemical forms in rats. Int J Radiat Biol 80:683–9.
616 doi: 10.1080/09553000400005486. PMID: 15586888

617 Fritsch P, Grappin L, Guillermin AM, Fottorino R, Ruffin M, Miele A (2007) Modelling of bioassay data
618 from a Pu wound treated by repeated DTPA perfusions: Biokinetics and dosimetric approaches.
619 Radiat Prot Dosim 127:120–4. https://doi.org/10.1093/RPD/NCM260

620 Fritsch P, Sérandour AL, Grémy O, Phan G, Tsapis N, Abram MC, et al. (2009) Simplified structure of a
621 new model to describe urinary excretion of plutonium after systemic, liver or pulmonary
622 contamination of rats associated with Ca-DTPA treatments. Radiat Res 171:674–86. doi:
623 10.1667/rr1530.1. PMID: 19580474

624 Fritsch P, Sérandour AL, Grémy O, Phan G, Tsapis N, Fattal E, et al. (2010) Structure of a single model
625 to describe plutonium and americium decorporation by DTPA treatments. Health Phys 99:553–9.
626 DOI: 10.1097/HP.0b013e3181c1cccd

627 Glover L, Bertelli L, Dumit S, Poudel D, Smith L, Waters T, Klumpp J (2022) Side effects and
628 complications associated with treating plutonium intakes: A retrospective review of the medical
629 records of LANL employees treated for plutonium intakes, with supplementary interviews. Health
630 Phys 123:348-359. doi: 10.1097/HP.0000000000001603

631 Gorden AEV, Xu J, Raymond KN, Durbin P, (2003) Chem. Rev. 103 4207. doi: 10.1021/cr990114x

632 Grappin L, Bérard P (2008) Autorisation de mise sur le marché du Ca-DTPA. Radioprotection. 43(3): p.
633 465-466. http://dx.doi.org/10.1051/radiopro:2008047. 43. 10.1051/radiopro:2008047

634 Grappin L, Bérard P, Beau P, Carbone L, Castagnet X, Courtay C, Le Goff J, Ménétrier F, Néron M and
635 Piechowski J (2006) Rapport CEA-R-6097.

636 Grappin L, Bérard P, Menetrier F, Carbone L, Courtay C, Castagnet X, Le Goff JP, Néron MO,
637 Piechowski J (2007) Radiat Prot Dosimetry. 127(1-4): p. 435-9. https://doi.org/10.1093/rpd/ncm296

638 Grappin L, Bérard P, Ménétrier F, Carbone L, Courtay C, Castagnet X, Le Goff JP, Néron MO, Beau P,
639 Piechowski J (2007) Radioprotection. 42(2): p. 163-196. doi:10.1051/radiopro:2006031

640 Grappin L, Legoff JP, Carbone L, Courtay C, Agrinier AL, Aninat M, Amabile JC, Florin A, Andre F (2009)
641 Radioprotection. 44(4): p. 447-461.

642 Grémy O, Blanchin N, Miccoli L (2021) Interpretation of enhanced fecal and urinary plutonium
643 excretion data under a 2-year regular DTPA treatment started months after intake. Health Phys
644 121:494-505. doi: 10.1097/HP.0000000000001458. PMID: 34591820; PMCID: PMC8505154

645 Grémy O, Blanchin N, Miccoli L (2022) Excretion of Pu-238 during Long-term Chelation Therapy by
646 Repeated DTPA Inhalation. Health Phys 123(3):197-207. doi: 10.1097/HP.0000000000001584. Epub
647 2022 May 20. PMID: 35613373

648 Grémy O, Laurent D, Coudert S, Griffiths NM, Miccoli L (2016) Decorporation of Pu/Am actinides by
649 chelation therapy: New arguments in favor of an intracellular component of DTPA action. Radiat Res
650 185(6):568–79. https://doi.org/10.1667/RR14193.1

651 Grémy O, Miccoli L (2019) Comments on "Improved modeling of plutonium-DTPA decorporation"
652 (Radiat. Res. 2019; 191:201-210). Radiat Res 192:680-681. doi: 10.1667/RR00OG.1. Epub 2019 Sep
653 26. PMID: 31556845

654 Hall RM, Poda GA, Fleming RR, Smith JA (1978) A mathematical model for estimation of plutonium in
655 the human body from urine data influenced by DTPA therapy. Health Phys 34:419–31. doi:
656 10.1097/00004032-197805000-00001. PMID: 711453

657 Hengé-Napoli MH, Stradling GN, Taylor DM (Eds.) (2000) Decorporation of radionuclides from the
658 human body, Radiat Prot Dosim 87 11:9–10. https://doi.org/10.1093/oxfordjournals.rpd.a032980

659 ICRP (2015) Occupational Intakes of Radionuclides: Part 1. ICRP Publication 130. Ann. ICRP 44(2):5-
660 188. doi: 10.1177/0146645315577539. Erratum in: Ann ICRP. 2016 Dec;45(3-4):350. Erratum in: Ann
661 ICRP. 2019 Dec;48(2-3):503. Erratum in: Ann ICRP. 2020 Dec 4;:146645320975548. Erratum in: Ann
662 ICRP. 2021 Jun 8;:1466453211013964. PMID: 26494836.)

663 ICRP (2016) The ICRP computational framework for internal dose assessment for reference adults:
664 specific absorbed fractions. ICRP Publication 133. Ann ICRP 45(2):5-73. doi:
665 10.1177/0146645316661077. Erratum in: Ann ICRP. 46(3-4):487. PMID: 29749258.

666 ICRP (2019) Occupational intakes of radionuclides: Part 4. ICRP Publication 141. Ann. ICRP 48(2/3):9-
667 501. https://doi.org/10.1177/0146645319834139)

668 James AC, Sasser LB, Stuit DB, Glover SE, Carbaugh EH (2007) USTUR whole body case 0269:
669 Demonstrating effectiveness of i.v. Ca-DTPA for Pu. Radiat Prot Dosim 127:449–55. doi:
670 10.1093/rpd/ncm473. Epub 2008 Jan 28. PMID: 18227077.

671 Jech JJ, Andersen BV, Heid KR (1972) Interpretation of human urinary excretion of plutonium for
672 cases treated with DTPA. Health Phys 22:787–92. doi:10.1097/00004032-197206000-00039

673 Jolly L, McClearen H, Poda GA, Walke W (1972) Treatment and evaluation of a plutonium-238 nitrate
674 contaminated puncture wound. Health Phys 23:333–341. doi: 10.1097/00004032-197209000-00007.
675 PMID: 4629952.

676 Kety SS (1942) The lead citrate complex ion and its role in the physiology and therapy of lead
677 poisoning. J Biol Chem 14:181-192. https://doi.org/10.1016/S0021-9258(18)72713-0

678 Konzen K, Brey R (2015) Development of the plutonium-DTPA biokinetic model. Health Phys
679 108:565–73. doi: 10.1097/HP.0000000000000283. PMID: 25905517

680 Konzen K, Brey R, Miller S (2016) Plutonium-DTPA model application with USTUR Case 0269. Health
681 Phys 110:59–65. doi: 10.1097/HP.0000000000000374. PMID: 26606066

LaBone TR (1994) HPS summer school on internal dosimetry: Evaluation of intakes of transuranics influenced by chelation therapy. Westinghouse Savannah River Company, Aiken (SC)

LaBone TR (2002) Health Physics summer school on internal dosimetry: A comparison of methods used to evaluate intakes of transuranics influenced by chelation therapy. Westinghouse Savannah River Company, Aiken (SC)

Lamart S, Van der Meeren A, Coudert S, Baglan N, Griffiths NM (2021) DTPA treatment of wound contamination in rats with americium: Evaluation of urinary profiles using STATBIODIS shows importance of prompt administration. Health Phys 120: 600-617. doi: 10.3389/fphar.2021.635792. PMID: 33841153; PMCID: PMC8032982.

Markley JF, Rosenthal MW, Lindenbaum A (1964) Distribution and removal of monomeric and polymeric Pu in rats and mice. Int J Radiat Biol 8:271–8. doi:10.1080/09553006414550281

Matthews EK (1986) CALCIUM AND MEMBRANE PERMEABILITY, British Medical Bulletin, Volume 42, Issue 4, 1986, Pages 391–397, https://doi.org/10.1093/oxfordjournals.bmb.a072157

Ménétrier F, Grappin L, Raynaud P, Courtay C, Wood R, Joussineau S, et al. (2005) Treatment of accidental intakes of plutonium and americium: guidance notes. Appl Radiat Isot 62:829–46. https://doi.org/10.1016/j.apradiso.2005.01.005

Norwood WD (1960) DTPA—effecttiveness in removing internally deposited plutonium from humans. J Occup Med 2:371–376. doi: 10.1097/00043764-196008000-00002. PMID: 14427692.

Ohlenschläger L, Schieferdecker H, Schmidt-Martin W (1978) Efficacy of Zn-DTPA and Ca-DTPA in removing plutonium from the human body. Health Phys 35:694–699.

Phan G, Ramounet-Le-Gall B (2004) Targeting of diethylene triamine pentaacetic acid encapsulated in liposomes to rat liver: an effective strategy to prevent bone deposition and increase urine elimination of plutonium in rats. Int J Radiat Biol 80(6), 413–422. doi: 10.1080/09553000410001702300. PMID: 15362694

Phan G, Ramounet-Le-Gall B, Deverre JR, Fattal E, Bénech H (2006) Predicting Plutonium Decorporation Efficacy after Intravenous Administration of DTPA Formulations: Study of Pharmacokinetic–Pharmacodynamic Relationships in Rats. Pharm Res 23. 2030-5. 10.1007/s11095-006-9046-x. doi: 10.1080/09553000410001702300. PMID: 15362694

Poudel D, Bertelli L, Klumpp JA, Waters TL (2017) Interpretation of urinary excretion data from plutonium wound cases treated with DTPA: Application of different models and approaches. Health Phys 113:30–40. doi: 10.1097/HP.0000000000000662. PMID: 28542009

Roedler HD, Nosske D, Ohlenschlager L, Schieferdecker H, Doerfel H, Renz K (1989) Incorporation of 241Am: Effectiveness of late DTPA chelation therapy. Radiat Prot Dosim 26:377–9. https://doi.org/10.1093/oxfordjournals.rpd.a080433

Romero PJ, Whittam R (1971) The control by internal calcium of membrane permeability to sodium and potassium. J Physiol 214(3):481-507. doi:10.1113/jphysiol.1971.sp009445

Schadilov AE (2010) Plutonium biokinetics following a wound injury and considering the effect of DTPA therapy. Dissertation. Moscow: Federal Medical and Biological Agency; (in Russian).

Schadilov AE, Khokhryakov VF, Kudryavtseva TI, Vostrotin VV (2005) Ca-DTPA effects on plutonium excretion from the human organism. Siberian Med J 2:128–132. (in Russian).

722 Schofield G, Lynn J (1973) A measure of the effectiveness of DTPA chelation therapy in cases of
723 plutonium inhalation and plutonium wounds. Health Phys 24:317–327. doi: 10.1097/00004032-
724 197303000-00007. PMID: 4691640.

725 Schubert J, Fried JF, Rosenthal MW, Lidenbaum A (1961) Tissue distribution of monomeric and
726 polymeric plutonium as modified by a chelating agent. Radiat Res 15:220–6. doi:10.2307/3571253

727 Serandour AL, Fritsch P (2008) Pulmonary retention of actinides after dissolution of PuO2 aerosols:
728 Interest in modelling DTPA decorporation. Radioprot 43(2):239–53. doi:10.1051/radiopro:2008004

729 Smith VH, Ballou JE, Clarke WJ, Thompson RC (1961) Effectiveness of DTPA in Removing Plutonium
730 from the Pig. Proceedings of the Society for Exp Biol Med 107(1):120-123. doi:10.3181/00379727-
731 107-26553

732 Stather JW, Smith H, Bailey MR, Birchall A, Bulman RA and Crawley FE (1983) The retention of 14C-
733 DTPA in human volunteers after inhalation or intravenous injection. Health Phys 22(6), 45–52.
734 https://doi.org/10.1097/00004032-198301000-00006

735 Stevens W, Bruenger FW, Atherton DR, Buster DS, Howerton G (1978) The retention and distribution
736 of 241Am and 65Zn, given as DTPA chelates in rats and of [14C]DTPA in rats and beagles. Radiat Res
737 75(2):397-409. PMID: 102009. https://doi.org/10.2307/3574913

738 Stradling GN, Hengé-Napoli MH, Paquet F, Poncy JL, Fritsch P, Taylor D (2000) Optimum treatment
739 regimens with animals. Radiat Protect Dosim 87:29–40.
740 http://dx.doi.org/10.1093/oxfordjournals.rpd.a032977

741 Taylor DM (1989) The biodistribution and toxicity of plutonium, americium and neptunium. Sci Total
742 Environ 83:217–25. doi: 10.1016/0048-9697(89)90094-6. PMID: 2781271.

743 Taylor DM, Hodgson SA, Stradling N (2007) Treatment of human contamination with plutonium and
744 americium: would orally administered Ca- or Zn-DTPA be effective? Radiat Prot Dosimetry 127(1-
745 4):469-71. doi: 10.1093/rpd/ncm299. Epub 2007 Jun 7. PMID: 17556346

746 Turner GA, Taylor DM (1968) The transport of plutonium, americium and curium in the blood of rats.
747 Phys Med Biol 13:535–546. doi:10.1088/0031-9155/13/4/304

748 Volf V (1978) Treatment of incorporated transuranium elements. IAEA Technical Reports Series No.
749 184 (Vienna: IAEA) (1978).

750 Volf V, Luz A, Schaffer E, Muller WA, Rencova J (1999) Effect of oral ZnDTPA on late effects of
751 injected plutonium in rat. Int J Radiat Biol 75:929–941. doi: 10.1080/095530099139692. PMID:
752 10465359

753 Wedeking P, Eaton S, Covell DG, Nair S, Tweedle MF, Eckelman EC (1990) Pharmacokinetic analysis
754 of blood distribution of intravenously administered ^{153}Gd-labelled Gd(DTPA)$^{2-}$ and ^{99M}Tc(DTPA) in rats.
755 J Magn Reson Imaging 8:567-575. https://doi.org/10.1016/0730-725X(90)90133-M

756